Investigation of Fouling in Perfusion Cell Culture Processes Using Alternating Tangential Flow Filtration

Veje, Malene Heilskov; Quirós, Manuel; Kristensen, Peter; Jørgensen, Mads Koustrup

Published in:
Journal of Membrane Science

DOI (link to publication from Publisher):
10.1016/j.memsci.2024.122764

Publication date:
2024

Document Version
Publisher's PDF, also known as Version of record

Journal of Membrane Science 701 (2024) 122764

Contents lists available at ScienceDirect

Journal of Membrane Science

journal homepage: www.elsevier.com/locate/memsci

Investigation of fouling in perfusion cell culture processes using alternating tangential flow filtration

Malene Heilskov Veje [a,b], Manuel Quirós [a], Peter Kristensen [c], Mads Koustrup Jørgensen [b,*]

[a] Novo Nordisk, Biotech and Rare Disease API Manufacturing Development, Gentofte, Denmark
[b] Aalborg University, Center for Membrane Technology, Department of Chemistry and Bioscience, Aalborg, Denmark
[c] Aalborg University, Department of Chemistry and Bioscience, Aalborg, Denmark

ARTICLE INFO

Keywords:
Fouling
Critical flux
Alternating tangential flow
Transmembrane pressure
Chinese hamster ovary cells

ABSTRACT

Microfiltration membranes are increasingly used to retain the cells inside bioreactors while continuous harvest of the desired biopharmaceutical occurs in perfusion processes. One method of microfiltration is Alternating Tangential Flow (ATF) filtration, which involves moving the cultivation broth tangentially back and forth across the membrane, which results in a backwash effect that reduces fouling. In this study, fouling was investigated with asymmetric polysulfone hollow fibers operated in ATF mode attached to a bioreactor producing a recombinant protein in Chinese Hamster Ovary (CHO) cells. Fouling was assessed through different approaches, including determination of critical flux using an improved flux-step method. Fouling was studied through measurements of Transmembrane Pressure (TMP), protein transmission, membrane pore size and staining of the membrane after operation to visualize the distribution of biological fouling inside the membrane. For critical flux determination, fluxes of up to 69 LMH were used without exceeding the critical flux. No sign of fouling was observed for the short-term (<3.5 h) critical flux experiment. However, during prolonged operation at 8.3 LMH the TMP jumped to 0.9–0.95 bar, indicating fouling. At this state, the protein transmission remains at the same high level (>88 %).

1. Introduction

Chinese Hamster Ovary (CHO) cells are the most common non-human mammalian cells used in the bioproduction of protein therapeutics (monoclonal antibodies (mAbs), recombinant proteins and peptides). According to Lu et al. [1], CHO cells lines are used in the production of up to 70 % of the protein therapeutics that have been approved since 2016. These cells are preferred because of their ability to grow in suspension cultures without the need of adhesion surfaces, allowing for an easier process scale-up [2,3], and their ability to perform human-like post-translational modifications (PTMs) [4]. In order to maximize the volumetric productivity, to reduce the residence time of the therapeutic protein in the bioreactor (which specially are of interest when producing labile products), and also to allow for smaller working volumes, perfusion bioreactors are increasingly being used in the pharmaceutical industry [5]. In a perfusion process, nutrients are continuously added, while the product and waste products are continuously removed, thus allowing higher cell densities to be maintained for longer durations. To make a perfusion process, a cell retention device is needed. Although devices such as spin filters or gravity settlers are available, Alternating Tangential Flow (ATF) or Tangential Flow Filtration (TFF) filters equipped with microfiltration membranes are today the most preferred cell retention devices in bioreactor perfusion processes. Microfiltration membranes are used as these will retain the mammalian cells in the reactor, as the cells have a diameter of 10–20 μm [6]. The recombinant protein, with a diameter in nanometer-range [7], can easily pass through the membrane. Typically, hollow fiber membranes will be used for cell retention device in perfusion processes. The membrane is operated in either ATF filtration or TFF mode [8]. In some studies, ATF has provided better transmission, compared to TFF [9–11]. The transmission is defined as the ratio of the concentration of the product in the harvest stream (membrane permeate, $C_{harvest}$) relative to the concentration of the product in the bioreactor (membrane feed, $C_{bioreactor}$) (Eq. (1)).

$$Transmission = \frac{C_{harvest}}{C_{bioreactor}} * 100\% \quad \text{Eq. 1}$$

In ATF filtration, a diaphragm pump is used to generate an

* Corresponding author.
E-mail address: mkj@bio.aau.dk (M.K. Jørgensen).

https://doi.org/10.1016/j.memsci.2024.122764
Received 2 February 2024; Received in revised form 3 April 2024; Accepted 8 April 2024
Available online 10 April 2024

alternating vacuum and pressure cycle, which in cycles will move the cultivation broth towards the membrane (pressure phase) and towards the bioreactor (exhaust phase), respectively, which is illustrated in Fig. 1. Therefore, the flow inside the membrane in the ATF mode will be reversed for each pressure-vacuum-cycle, in contrast to TFF which use a unidirectional flow [8,11]. It has been suggested that the alternating crossflow generates a backflushing effect which contribute to decreasing the deposition of biomaterial on the membrane [12], and thereby allowing for higher transmission in ATF compared to TFF [9,10]. Radoniqi et al. [13] has shown that the backwash effect was present at the outlet of the ATF filter using computational fluid dynamic modeling [13], meaning that the backwash effect will be more pronounced at the top of the filter during the pressure phase, and at the bottom of the filter during the exhaust phase [12].

Independently of which membrane operational mode is used, the membranes are prone to fouling [11], which can reduce the permeate flux and transmission, thereby reducing productivity [14]. Apart from the decreased productivity, a fouled membrane can also negatively affect the cell culture as retained waste products may be toxic for the cells, when present at high concentration. The influence of membrane fouling on the permeate flux can be seen in Eq. (2) and Eq. (3) [15,16].

$$J = \frac{\mathrm{TMP}}{\mu \cdot R_t} \quad \text{Eq. 2}$$

$$R_t = R_m + R_{rev} + R_{irrev} \quad \text{Eq. 3}$$

Where J is the permeate flux, TMP is the transmembrane pressure, μ is the viscosity of the permeate, R_t is the total resistance of the membrane filtration, R_m is the inherent resistance of the membrane, R_{rev} is reversible fouling, and R_{irrev} is irreversible fouling which only can be removed through chemical cleaning. From Eq. (2) it can be seen that when the total resistance, due to fouling and/or cake formation, increases it will result in either a decrease in flux or an increase in TMP when operating at constant pressure and flux, respectively [15]. When fouling occurs, the flux will not be linearly dependent on the TMP. This point is defined as the critical flux and indicate the onset of fouling [16,17]. The original hypothesis behind critical flux theory was that when operating with a flux below the critical flux, fouling will not be observed in short-term filtrations, and therefore theoretically flux decline should not be observed [18]. Therefore, operating below the critical flux is favorable both economically and environmentally. One method to investigate the critical flux is to use the improved flux-step method, which was described by Marel et al. [19]. Here the flux is increased in steps and afterwards decreased in steps again. Between each step, a relaxation flux is applied, therefore allowing both the critical flux and reversibility of the fouling to be measured in a single experiment. For fluxes below the critical flux, the TMP will be constant throughout the step [19].

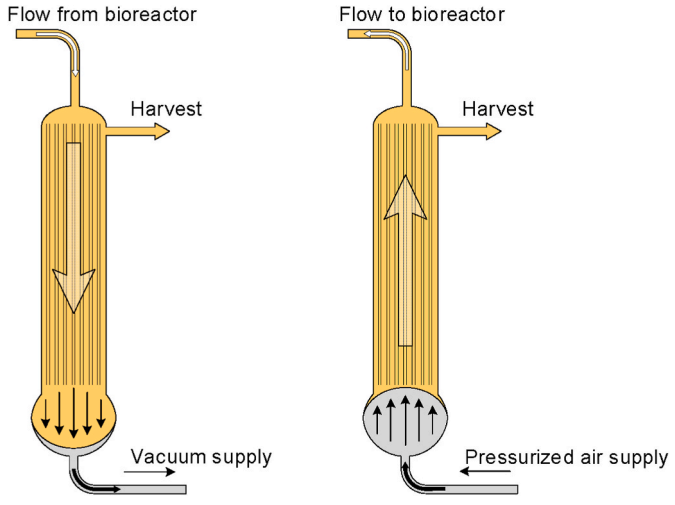

Fig. 1. Working Principle of Alternating Tangential Flow Filtration. The left figure illustrates the exhaust phase, and the right figure illustrates the pressure phase.

In this study ATF filtration was studied to understand the fouling of the cell retention membrane filter in mammalian cell cultivation. This was done by systematic analysis of the short-term membrane fouling by the improved flux-step method to assess the critical flux, along with long-term filtrations during cell cultivation. To the authors knowledge critical flux experiments have not been conducted on ATF filtrations before, however this approach is typically used for TFF processes, and specially also for scaling up TFF membrane filtration processes [20]. The fouling of the membrane was monitored by protein transmission, and by continuous TMP measurements during the constant flux perfusion process. To the authors knowledge, no TMP measurement, which gives critical information about fouling, has been published for a system similar to this, with the same membrane type and configuration. Additionally, the fouling was characterized after the end of the cultivation by measuring the pore size distribution of the membrane and by staining of the membrane with hematoxylin and thionine. The staining will be used as a method to visualize the biological fouling distribution inside the membrane.

2. Material and methods

2.1. System setup

Fouling was investigated using CHO cell cultivation broth. The bioreactor was connected to BioStat® B-DCU (Sartorius) fermentor. Two membranes were mounted on the bioreactor (see Fig. 2) but only one were active at a time. So, when the first membrane was fouled, the next membrane was used. The membranes used were BioOptimal™ MF-SL

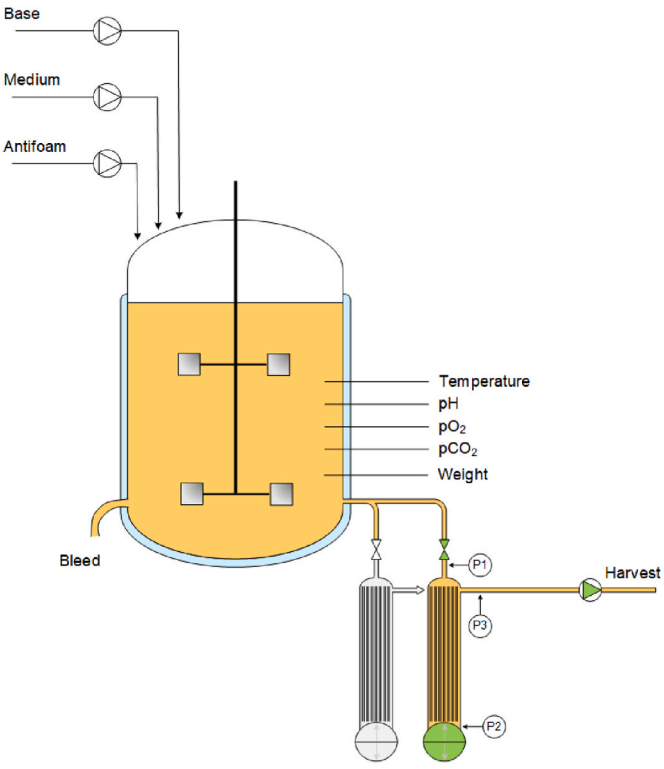

Fig. 2. Schematic diagram of the setup for the experiments. Base, medium and antifoam is added. The temperature, pH, pO_2, pCO_2 and weight of the reactor is controlled. The white membrane is stand-by and will be used when the green membrane is fouled. (For interpretation of the references to color in this figure legend, the reader is referred to the Web version of this article.)

Microfilters hollow fibers (Asahi Kasei) which are asymmetric polysulfone (PS) membranes with a nominal pore size of 0.4 μm [21]. The membrane modules were custom-made with a membrane area of 0.025 m^2. The modules have 9 fibres, the length of the fibres was 65 cm, and the inner radius was 0.7 mm. Before use, the membranes were washed with water to eliminate the 20 % ethanol preservation solution. The membranes were operated as inside-out hollow fibers in ATF mode. A diaphragm pump, controlled by XCell TM ATF System C24 controller (Repligen), was used to generate the alternating crossflow in the membrane module. An XCell ATF® 2 Stainless Steel Device (Repligen) with a displacement volume of 0.1 L was used and the ATF rate was set to 0.8 L/min, corresponding to a cycle time of 7.5 s, and a shear rate of 5500 s^{-1} at the inner wall, assuming linear pipe flow and Newtonian fluid (calculated from Eq. (4) [22]).

$$\dot{\gamma} = \frac{8v}{D} = \frac{4Q}{\pi r^3} \quad \text{Eq. 4}$$

where v is the fluid velocity, D is the diameter of the pipe, Q is the flow and r is the inner diameter. For the ATF system Q can be calculated by the ATF rate divided by the number of fibers in the membrane.

A pump from the BioStat® B-DCU setup was applied on the permeate side to draw broth from the membrane feed to the permeate side of the membrane. For both membranes, three pressure transmitters were mounted. The pressure transmitter used to measure the pressure on the permeate side was PREPS-N-038 (Pendotech) while the pressure transmitters on the feed side of the membrane were PREPS-N-5-5 (Pendotech). All pressure transmitters were connected to an LCO-i100 controller (Levitronix GmbH Switzerland) for data collection. The pressure transmitters were used without further calibration than obtained from the manufacturer. During the critical flux experiments the pressure was collected at least every 0.3 s, while the pressure during the rest of the cultivation time was collected each 5 s.

2.2. Perfusion culture

CHO cells producing a recombinant protein with a molecular weight of approximately 60 kDa were used for this study. The growth medium used was chemical defined. The seed train was started from a working cell bank ampoule from Novo Nordisk. The cells were thawed and transferred to shake flasks of increasing volume for one week in an incubator and were afterwards transferred to the bioreactor. The working volume, harvest rate and bleed rate were gravimetrically controlled, and the working volume was kept constant. The general operation conditions (e.g. flux, setpoints for pH, pCO_2, pO_2, temperature) were selected based on a process characterization study that investigated the impact of the main process parameters on product titer and quality. The ranges of the parameters investigated were established based both on previous process knowledge and capacity at the manufacturing site. The harvest was started on day 3 with a flux of 4.3 LMH and was increased to 8.3 LMH on day 4. A pulsed bleed was applied 10 min each hour in order to maintain a high viability throughout the cultivation. The pH was controlled by addition of CO_2 gas through the ring sparger, and addition of 10 % Na_2CO_3. The pCO_2 was controlled by addition of air through the ring sparger. Dissolved oxygen was controlled through addition of O_2 through the microsparger. HyClone, 10 % ADCF Antifoam solution (Cytiva) was added when needed in order to reduce foam levels to a few centimeters. The pH and pCO_2 were monitored continuously inline and monitored offline once per day. Based on offline measurement the pH was recalibrated when deviating more than 0.05, and the pCO_2 probe was recalibrated when deviating more than 10 mmHg. Dissolved oxygen was only measured inline and was therefore not recalibrated.

2.3. Critical flux

The experiment was conducted in two replicates, referred to as Exp 1 and Exp 2 in the rest of this manuscript. Critical flux experiments were conducted using an improved flux-step method [19]. This method has earlier been applied for TFF setups, but will in this manuscript be applied for the ATF setup. In the current study, the flux was gradually increased in steps and are afterwards lowered in steps again. The steps were kept for 1.5–15 min, and have fluxes of approximately 0.5, 1, 2, 5, 10, 20, 40 and 69 LMH. Between each flux step a relaxation flux of 0.1 LMH was kept for 3–5 min. For each replicate experiment, two individual critical flux experiments were conducted. The first critical flux experiment was conducted in the cell culture medium before inoculation, while the second experiment was conducted when the cell density approached a maximum. All critical flux experiments were conducted on clean membranes which have not been used before. For each step the average, maximum and minimum TMP was calculated. For the critical flux experiments the flux was manually adjusted using an external peristaltic pump (Watson-Marlow) to control the permeate flow. The TMP was calculated using Eq. (5), where P_1 and P_2 are the inlet and outlet pressure of the membrane, and P_3 is the pressure on the permeate side of the membrane, as illustrated in Fig. 2.

$$TMP = \frac{P_1 + P_2}{2} - P_3 \quad \text{Eq. 5}$$

2.4. Samples analyses

Samples were collected once daily from both the harvest and bioreactor. For the bioreactor sample the pH and pCO_2 were checked offline using a Rapid Point 500e (Siemens Healthineers) while viable cell density (VCD), viability and cell diameter were monitored with Cedex HiRes (Roche). The bioreactor sample was then centrifuged at 2432×g for 100 s in a Sigma 2–6 Compact Centrifuge. The supernatant was then analyzed for cultivation metabolites using using a Bioprofile 100 Plus (Nova Biomedicals) for Exp 1, and using Nova Bioprofile Flex2 (Nova Biomedicals) for Exp 2. For the harvest sample, the harvest pump was turned off, and the harvest sample was collected from the harvest bag via the harvest line. The harvest bag was kept at 4 °C and replaced each third day. The harvest and bioreactor samples were filtered through a PVDF 0.22 μm syringe filter and stored at −20 °C until concentration measurements of the recombinant protein. The concentration of the recombinant protein was analyzed both for harvest and bioreactor material using a High-Performance Liquid Chromatography (HPLC)-method based on an affinity column that binds the produced recombinant protein. The HPLC samples were analyzed using a e2695 Separation module from Waters with a 2474 FLR Detector. The transmission was calculated according to Eq. (1).

2.5. Staining

In order to visualize the biological fouling distribution inside the membrane, different dyes were used. The membranes were stained with Mayer' Hematoxylin Solution (Sigma) and 1.3 % Thionine, respectively. Hematoxylin stain nucleic acids blue, and thereby the cell nuclei will be stained blue [23]. Thionine is a basic dye, which binds to nucleic acids [24]. Initially, approximately 2 cm of a clean and a fouled membrane from close to the harvest line was cut. Each piece was then sectioned into two pieces; one for hematoxylin stain and one for thionine stain. For the thionine samples, the membrane pieces were placed in the thionine staining solution for approximately 4 min. Afterwards the excess dye was removed by putting the fiber into a water bath. The thioine-stained and the none-stained membrane pieces were embedded in OCT Mounting media (VWR chemicals) and was afterwards sectioned by freezing microtome (Leica CM3050 S Cryostat) in sections of 5 μm. The sections were collected on SuperFrost®, Microscope Slides (VWR).

Afterwards the none-stained membrane slices were stained with hematoxylin stain. The staining was applied with incubation time of 5 min, and afterwards followed by rinsing with water. Both the hematoxylin and thionine samples were afterwards analyzed with Olympus BX 43 microscope.

2.6. Pore size distribution

The nominal pore size of the membrane is indicated by the manufacturer to be 0.4 μm [21], however, analysis of the pore size distribution of a clean and fouled membrane was carried out in order to quantitatively measure fouling impact on pore size. The pore size of the membranes was measured using Porolux 1000™ porometer with the measuring mode full porometry and using the step method. The gas used was N_2, while the wetting liquid was Porefil™. The measurement is based on calculations which assume shape factor of 0.715. The pressure was varied between 0 and 2 bar, and 20 measurements were made for the wet curve and 7 measurements for the dry curve. A cut of approximately 10 cm of the membrane was used for this analysis, and the end of the fiber was closed with two-component epoxy.

3. Results

3.1. Cell culture

The viability, defined as the percentage of living cells of the total cells, and VCD can be seen in Fig. 3 for both Exp 1 and Exp 2. The VCD increases until day 8, and afterwards a steady state is kept. The average cell diameter can be seen in Fig. 4, for both Exp 1 and Exp 2. The cell parameters, including viability, VCD and average cell diameter were quite similar for both experiments. For Exp 1 the bleed was, due to a mistake, started after 109 h instead of the planned 96 h, which partly explains the difference in VCD measured on day 5. The measured metabolites were quite similar for Exp 1 and Exp 2 (data not shown).

3.2. Short-term fouling potential

The short-term fouling potential was investigated using the improved flux-step method for critical flux determination. The critical flux experiment at high cell density, corresponding to close to maximal VCD, was conducted after 8.7 days for Exp 1 and after 7.9 days for Exp 2. The results for the critical flux experiments can be seen in Fig. 5. The TMP values shown in Fig. 5 are relative to the smallest TMP measured for that experiment. In Fig. 5 only the relative minimum, maximum and average TMP is plotted for each flux step, however it should be noted that for each step the wave pressure curves had similar frequency, amplitude, crest and trough in all the period for each flux step. This applies to all the pressure transmitters. An example of the pressure curves for the complete flux step of 69 LMH, for Exp 2, can be seen in Fig. S - 1. Further Fig. S – 2 in the supplementary material contains graphs that shows the flux and the average TMP shown in Fig. 5 with a properly scaled axis for the average TMP. In Fig. 5 it should be noticed that the critical flux experiment for Exp 1 in cell culture medium (Fig. 5a) was conducted with ATF rate of 0.4 L/min in contrast to 5b, 5c and 5d, which was conducted with ATF rate 0.8 L/min. Further it should be observed that the maximal flux in the same experiment (Fig. 5a) was lower compared to the rest of the critical flux experiments seen in Fig. 5. It was decided to increase the maximal flux for the rest of the experiments as only a very limited increase in TMP was observed at the maximal flux of 38.5 LMH, as seen in Fig. 5a. For Fig. 5b, c and 5d the maximal rotation speed of the external pump was therefore used to achieve a flux of approximately 69 LMH for the maximal flux step. For Fig. 5d the difference on the maximal and minimal TMP is larger compared to Fig. 5a, b, and 5c, and therefore the scale on the secondary y-axis is also different compared to Fig. 5a, b, and 5c. However, similar trend with increasing pressure for increasing flux is seen in for this experiment (see Fig. S – 2). The large difference in minimum and maximum TMP observed in Fig. 5d is a result of the pressure in this experiment being collected on 2 different consoles, and therefore there was a slightly difference in timing for the collected pressure data. As the pressure measurements were collected each 0.3 s, the alternating pressure curves were easily identified and therefore it was possible to manual shift the curves, so they overlap as good as possible. However, there will still be a very small difference, resulting in some points that are not completely aligned. The manually alignment was conducted for each flux step by shifting rows, without deletion of datapoints. An example of raw data (from time between 95 and 105 min in Fig. 5c) and the manually shifted data can be seen in Fig. S - 1.

Another way to visualize the data from the short-term fouling (Fig. 5) is to correlate the flux and the average TMP. For fluxes above 5 LMH, a linear correlation was found ($R^2 > 0.85$). The permeability in LMH/bar, corresponding to the slope for the linear regression of the flux against the average TMP is illustrated in Fig. 6. For the full dataset for all flux steps, see Fig. S - 3. As there is linear relationship between TMP and flux, the critical flux has not been exceeded, and the short-term fouling potential is therefore low. The critical flux experiments at high cell density have a lower permeability (Fig. 6) compared to critical flux experiments conducted with cell culture medium, indicating increased viscosity or an effect on the boundary layer which impedes the flux when filtering the cell cultivation broth.

3.3. Long-term fouling filtration

The long-term fouling was investigated using TMP and transmission measurements. The average TMP, calculated for each 2 h, can be seen in Fig. 7a and b for Exp 1 and Exp 2 respectively.

The concentration of the recombinant protein in the bioreactor and harvest was measured using HPLC. For both the bioreactor and the

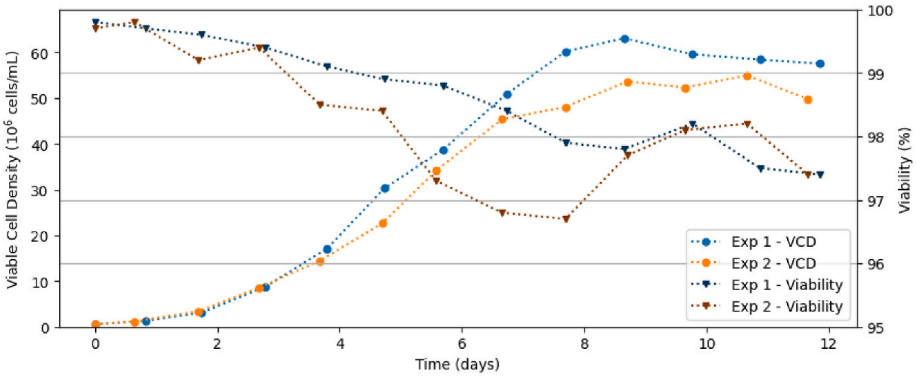

Fig. 3. Viable Cell Density and viability for experiment 1 and 2.

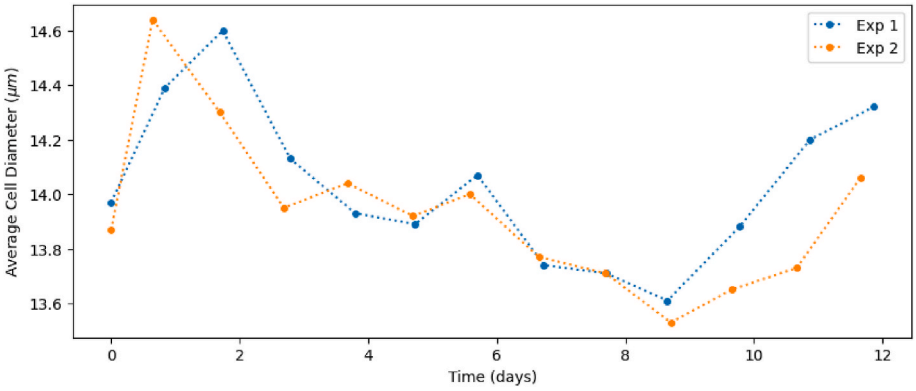

Fig. 4. Average cell diameter for experiment 1 and 2.

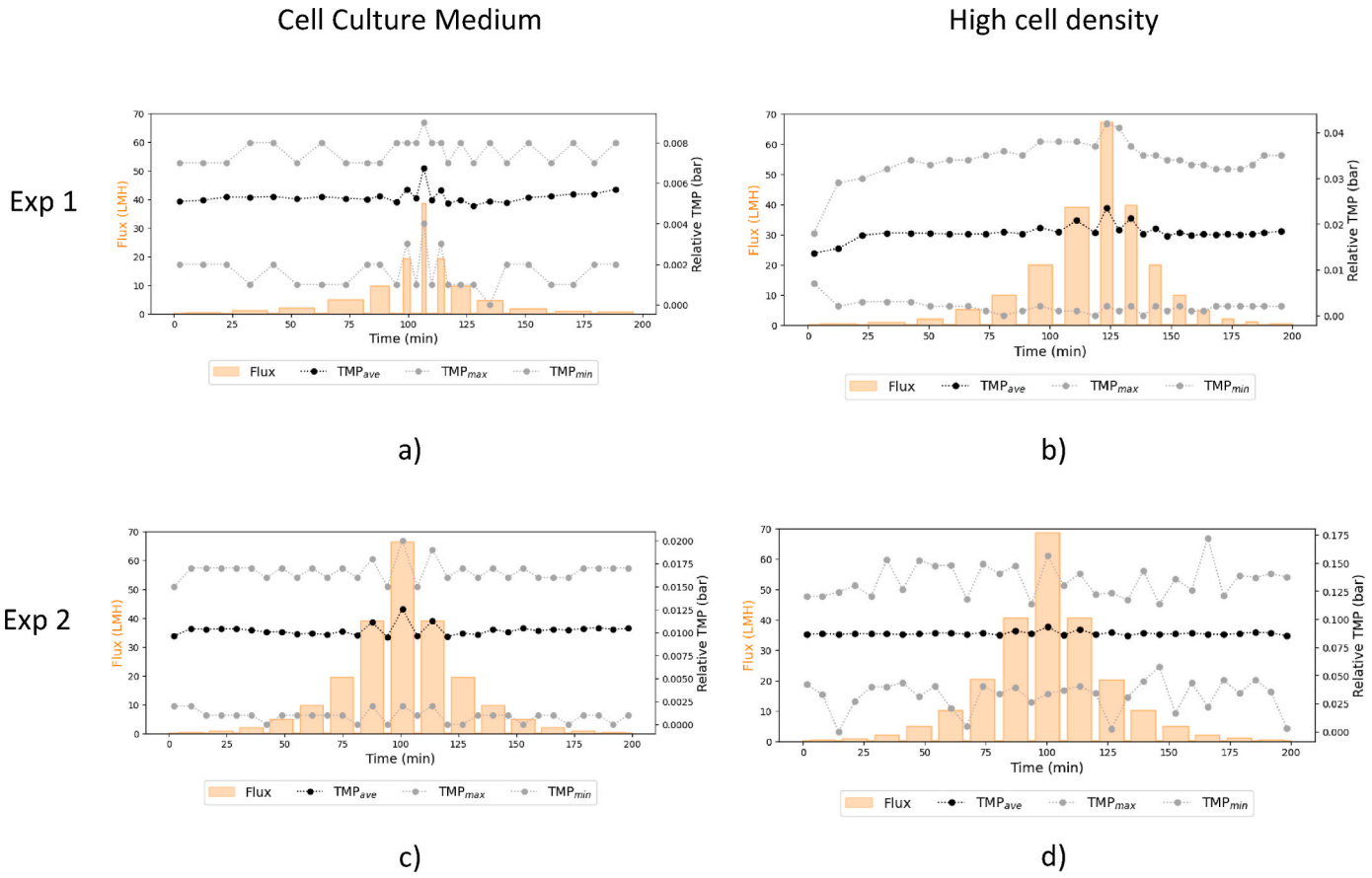

Fig. 5. Critical flux experiments. The graphs showing the flux (left y-axis) and the relative minimum, maximum, and average TMP (right y-axis) against the time for each experiment. a) Exp 1, membrane 1, in cell culture medium, ATF rate = 0.4 L/min b) Exp 1, membrane 2 at high cell density, ATF rate = 0.8 L/min c) Exp 2, membrane 1, in cell culture medium, ATF rate = 0.8 L/min d) Exp 2, membrane 2 at high cell density, ATF rate = 0.8 L/min.

harvest sample, the concentration of the recombinant protein was in the mg/L range. From the concentrations the transmission of the recombinant protein can be calculated using Eq. (1). The transmission for Exp 1 and Exp 2 are shown in Fig. 8. Here it can be seen that transmission remains constant between 88 and 97 % when looking at the transmission for day 7.5 and forward. For both Exp 1 and Exp 2, the transmission and harvest concentration seem lower than expected on day 7. To investigate the reproducibility of the protein concentration measurements, some samples were measured and similar results were obtained thus confirming the reproducibility. From both a biological and filtration point of view, no explanation for the sudden drop in transmission can be found as no active change was made to the system. It could possibly be explained by wrong handling or analysis of samples. No explanation can be found in the metabolic data (data not shown), where metabolites are as expected. If making linear interpretation for the concentration in both harvest and bioreactor, based on the sample at day 6 and 8, the transmission on day 7 can be recalculated to 94 % and 82 % for Exp 1 and Exp 2. The lower transmission for day 4 is likely due to being close to the quantification level for the HPLC-method.

3.4. Membrane autopsy

After operation the pore size of the membrane was measured. For a clean membrane the dominating pore size was 0.30 μm which

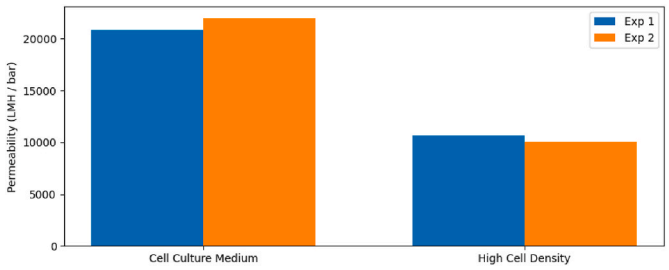

Fig. 6. Permeability for each experiment, based on linear regression for flux versus TMP for flux >5 LMH measured during the critical flux experiments in cell culture medium and at high cell density.

constitutes for 94 % of the total pore area, while for the fouled membrane 2 from Exp 2 it was 0.26 μm and 79 %. The full results from the porosity measurement can be found in Fig. S – 4. The lower dominating pore size for the used membrane is an indication of fouling. It should be noted that this is a single determination, and only a small section of the membrane.

Besides the quantitative pore size measurement, a qualitative determination of fouling was carried out using staining of the membranes. The hematoxylin stain can be seen in Fig. 9, while the thionine stain can be seen in Fig. 10. From Fig. 9a, it can be seen that an unused membrane does not contain any particulate cellular matter, as there is very little staining observed, while it is clear that the used membrane contain significant amounts of cellular material indicated by the positive hematoxylin stain, which can be seen Fig. 9b. A zoom (Fig. 9c) highlights that intact cell, indicated with the intense blue color as the cell nucleus, only are located in the upper layer of the membrane. For the thionine stain it was seen that an unused membrane (Fig. 10a) shows a very limited amount of intense stained flake-like structures, while the rest of the membrane did not absorb the staining. In Fig. 10 b it is clear that the different areas in the membrane (indicated by arrows) are stained with different intensity, indicating different amount and/or type of fouling.

4. Discussion

By enhancing the understanding of the fouling process in a perfusion cell culture process it could be possible to increase the productivity, e.g., by increased transmission of the protein through the membrane, changing the flux or by prolonging the operational time of the membrane. The increased productivity will lead to both economic and environmental benefits. Retainment of inhibitory factors by the membrane could potentially have a negative impact on the cell culture. Hence, understanding fouling mechanisms would also be valuable from a biological perspective as well.

4.1. Short-term effects

The manufacturer of the membrane indicate that the water permeability is ≥ 21.000 LMH/bar at 25 °C. This corresponds well with the permeability for filtration in cell culture medium which was 20.852 LMH/bar for Exp 1 and 21.981 LMH/bar for Exp 2 (Fig. 6), while the permeability for the high cell density experiments (Fig. 6) are lower (10.697 LMH/bar for Exp 1 and 10.050 LMH/bar for Exp 2, see Fig. 6), which indicate an increased viscosity and/or resistance from fouling or concentration polarization. The linear trend for flux versus the average

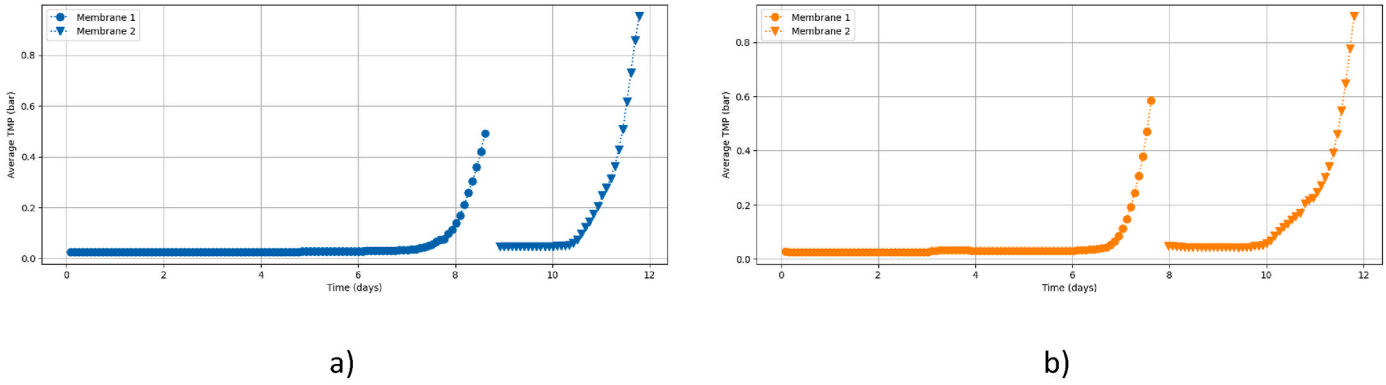

Fig. 7. a) Average transmembrane pressure (TMP) calculated for each 2 h for Exp 1, and b) average TMP for Exp 2.

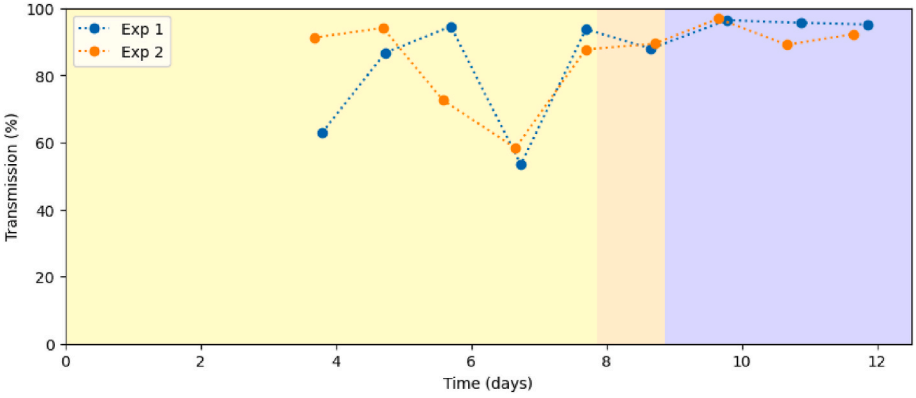

Fig. 8. Transmission. The yellow part indicates that membrane 1 is used for both Exp 1 and Exp 2, for the orange part membrane 1 is used for Exp 1, while membrane 2 is used for Exp 2, and for the blue part membrane 2 is used both for Exp 1 and Exp 2. (For interpretation of the references to color in this figure legend, the reader is referred to the Web version of this article.)

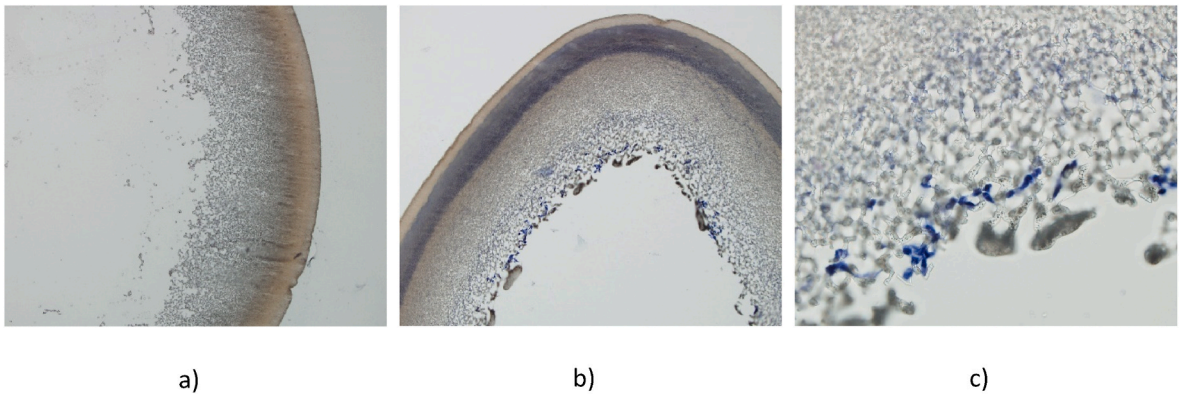

Fig. 9. Hematoxylin staining of membranes and analyzed by light microscope. a) Unused membrane filter, 100x b) Membrane 2 from Exp 2, 100x. C) Membrane 2 from Exp 2, 400x.

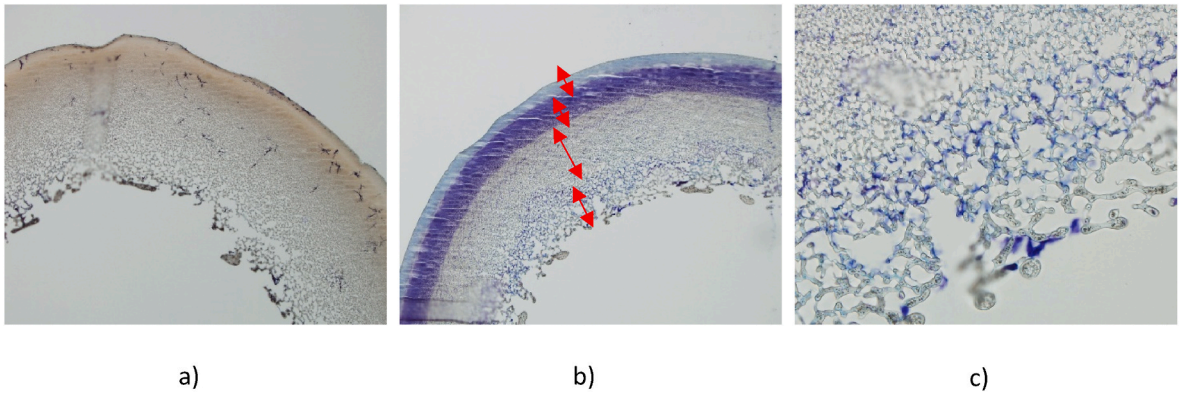

Fig. 10. Thionine staining of membranes and analyzed by light microscope. a) Unused membrane filter, 100x b) Membrane 2 from Exp 2, 100x. The red arrows indicate different regions of the membrane with different staining intensity. c) Membrane 2 from Exp 2, 400x. (For interpretation of the references to color in this figure legend, the reader is referred to the Web version of this article.)

TMP for both cell culture medium and high cell density (Fig. S - 3) indicate that the critical flux has not been exceeded. This is further supported by that the average TMP was constant throughout all the period for each flux step (complete data not shown, an example for complete data for the critical flux step of 69 LMH in Fig. 5d is shown in Fig. S - 1). For all the critical flux experiments, both in cell culture medium and at high cell density, only reversible fouling was observed as the average TMP for each flux step was similar for both the step-up and the step-down periods (Fig. S - 7). For cell culture medium this could be expected as the cell culture medium is sterile filtered before the critical flux testing, and therefore most of potentially fouling components should have been removed. For high cell density similar trend is observed, which however is more unexpected as e.g. cells, cell debris, and antifoam would be expected to contribute to fouling. However, there is not observed any significant fouling from these in the flux step experiments.

4.2. Long-term effects

The long-term effect of fouling can be seen from the increasing TMP in Fig. 7. To the authors knowledge no TMP measurement has been published in a system similar to this with same the membrane type and configuration, and therefore it is difficult to compare with previous studies. A study have previously measured TMP during their cultivation with hollow fibers in TFF mode, however their conditions are not comparable to the parameters used in this study [25]. Another study has measured the TMP, but have however not published how the TMP develops over time in their ATF perfusion process [26]. In the current study, very similar TMP profiles were observed for the two replicates. For both experiments, membrane 2 was exposed to a significant amount of fouling which causes an increase in TMP to 0.9–0.95 bar at the end of the experiment, and that the permeate pump was unable to reach the harvest rate setpoint. From Fig. 7 it can be seen that the operational time of the membranes were 5.9 days and 2.9 days for membrane 1 and 2 respectively for Exp 1, while it were 5.0 days and 3.8 days for Exp 2, when taking into account that the harvest was first started on day 3. Here it should also be kept in mind that the first day for membrane 1 was with half of the flux compared to the rest of the days, and therefore the membrane was less stressed in this period. It should further be noted that the end TMP for membrane 1 was significantly lower compared to membrane 2 for both experiments, meaning that that the operational time of membrane 1 could have been extended before reaching the same degree of fouling as seen for membrane 2. Another way to compare the membrane performance is with the filter capacity in relation to filtered volume per membrane area (Fig. S – 8). Here it was seen that for both Exp 1 and Exp 2 the filter capacity was larger for membrane 1 compared to membrane 2. This would in general be expected as membrane 2 is more stressed compared to membrane 1. Some parameters which are suggested to influence this is that the average flux is larger, there is more antifoam added, a higher protein concentration, higher VCD and likely also higher amount of cell debris, all factors that potentially could contribute to fouling. Further, the aggregate rate, meaning the percentage of counted cells that are present in aggregates increases from approximately 5 % to 36–50 % from the start of the cultivation to the end of the cultivation (data measured with Cedex HiRes, not shown in this manuscript), which potentially also influence the fouling

mechanism. In this study the accumulated amount of viable retained cells, calculated as the VCD times the harvest volume for different timesteps, does not directly correlate with the increase in TMP (data not shown in this manuscript). This indicated that the amount of viable retained cells, indirectly influenced by the VCD, alone cannot explain the difference in filter capacity for the membranes used in this study. The complexity of the fouling in this system is also highlighted by the fact that the filter capacity (Fig. S – 8) for membrane 1 and membrane 2 for Exp 1 were very different, while the filter capacity for membrane 1 and membrane 2 in Exp 2 were more similar, even though for both experiments the measured values, including bleed rate, harvest rate, metabolites, VCD, viability, average cell diameter and transmission, were quite similar. Therefore, it is expected that a more complex combination of the biological parameters is involved in the fouling mechanism, which is not fully understood yet.

As described, no irreversible fouling was observed in the critical flux experiments, however irreversible fouling was observed in the long-term-effects. When sampling from the harvest line, the harvest pump was turned off, and therefore the TMP was briefly lowered while the ATF-crossflow was still running, thereby possibly removing reversible fouling. However, there was not a clear effect from this when looking at the average pressure 30 min before and after sampling (see Fig. S - 6). It should however be kept in mind that the TMP was only lowered for approximately 1 min, so the effect of sweeping away reversible fouling could perhaps be seen if the lower TMP, and ATF-crossflow was kept for a longer duration. While the observed long-term fouling in this study was irreversible, another study investigating fouling with mammalian cells in a TFF-setup [25] suggested that approximately 75 % of the fouling observed in their 5-day experiment was reversible, however the conditions used in that study are not comparable to the conditions in the current study. In relation to transmission, no sign of fouling was observed as the transmission remains above 88 % even though the TMP increased, and ultimately the flux also declined slightly in the last hours of the cultivation. Importantly, the transmission is calculated from a harvest sample taken from the harvest bag. The concentration of the recombinant protein in the harvest bag would likely be lower than if the sample was taken directly from the harvest line, due to dilution with harvest from the earlier days, with a lower recombinant protein concentration, due to the lower VCD in the earlier days.). Based on this the actual transmission of the protein through the membrane would therefore be expected to be even higher than the transmission measured and shown in this study. A possible explanation for the high transmission is the asymmetric structure of the membrane. It has been suggested that it can be beneficial to have a thin secondary membrane, which can lead to higher stable transmission and flux [27]. When the open structured side of the membrane is facing the membrane feed stream it is suggested that the fouling layer formed inside the porous pore structure, will be less dense compared to if it was formed above the membrane surface [28].

In this study the cultivation time was shorter compared to other typical studies in this field [8,29–31]. In this study the experiment was terminated due to the fouled membrane, since the targeted harvest rate could not be maintained. Similar fouling phenomena with the same membrane and cell line has been seen in manufacturing scale, and thereby verify results shown in this manuscript. A factor that likely influences the fast fouling of the membrane is that a flux of 8.3 LMH has been used in this study. This is very high compared to typical flux values reported in this area which is 2–3 LMH [8]. Due to limitations in the experimental setup, a very high crossflow, and therefore a high shear rate of 5500 s^{-1} has been used. This likely also influence the membrane filtration process, as is has been shown that shear, induced by a peristaltic pump, increase the cell lysis, which partly contributes to lower transmission [11]. Another factor that can contribute to fouling is deposited antifoam micelles and cells on the membrane, which was investigated by Kelly et al. [32]. For the current study the exact amount of antifoam has not been monitored for Exp 1 but for Exp 2 the amount of added antifoam was 24 mL for the cultivation (the dosing profile can be seen in Fig. S - 5).

4.3. Staining

The stained membranes (Figs. 9 and 10) showed that intact cells were only located in the very inner layer of the membrane at the lumen side of the fiber. The staining also revealed that other compounds were stained in the depth of the membrane. Here different regions were stained with different intensity indicating different type and/or amount of fouling. Another study [27], working with CHO cells and the same type of membrane, BioOptimal MF-SL microfiltration membrane, in TFF-mode observed, using confocal laser scanning microscopy and staining, that an large amount of DNA and protein was in the depth of approximately 50 μm from the membrane surface, while the outer membrane layer did not have DNA but had some protein. It was indicated that intact cells can be found in upper 50 μm layer where both protein and DNA is present – this is different from the current study where intact cells are only seen in the very upper layer of the membrane, and are therefore not present in the depth of the membrane. Another study [33] using CHO-cells in an ATF perfusion process did not observe any distinct cells on the membrane surface using SEM but suggested that it is possible that these were flushed away before fixing with glutaraldehyde. The results in the current study indicate that fouling occurs across the depth of membrane, however the exact fouling components remain unknown. A possible method to investigate this further is to use other staining techniques, e.g. a general protein stain, or a stain specific for the produced recombinant protein, or possibly quantitative methods like Energy-dispersive X-ray spectroscopy (EDX).

5. Conclusion

In this study fouling was investigated in a reverse asymmetric hollow fiber membrane. CHO cell containing cultivation broth was used as membrane feed solution, and the membrane was operated in ATF-mode. Fluxes of up to 69 LMH was used in critical flux experiments, without exceeding the critical flux. No irreversible fouling was observed for the critical flux experiments, and further it was observed that a higher resistance and/or viscosity was present when filtering the cell containing cultivation broth compared to cell culture medium. When operating at a prolonged time at a flux of 8.3 LMH significant fouling was observed. When the TMP reached 0.9–0.95 bar, the permeate pump was not able to reach the harvest setpoint due to fouling, and the flux therefore started to decline. The transmission for the recombinant protein was not observed to decrease despite the large amount of membrane fouling. The fouling of the membrane was quantified by pore size measurements, where the dominating pore size of a clean and a fouled membrane was 0.30 μm and 0.26 μm, respectively, indicating fouling. Further, fouling was proven by staining of the membrane. Here all the depth of the membrane was stained, however with different intensity indicating different amount and/or type of fouling. Intact cells were only observed in the very upper layer of the membrane facing the cultivation broth (feed solution).

CRediT authorship contribution statement

Malene Heilskov Veje: Writing – original draft, Visualization, Methodology, Investigation, Formal analysis. **Manuel Quirós:** Writing – review & editing, Supervision. **Peter Kristensen:** Writing – review & editing. **Mads Koustrup Jørgensen:** Writing – review & editing, Supervision, Conceptualization.

Declaration of competing interest

The authors declare the following financial interests/personal relationships which may be considered as potential competing interests: Malene Veje reports equipment, drugs, or supplies was provided by

Asahi Kasei Corp. If there are other authors, they declare that they have no known competing financial interests or personal relationships that could have appeared to influence the work reported in this paper.

Data availability

Data will be made available on request.

Acknowledgement

The authors would like to thank Novo Nordisk, department 2299, for conducting the HPLC analysis as well as Novo Nordisk, department 4284, for assistance with cryomicrotome and staining.

Appendix A. Supplementary data

Supplementary data to this article can be found online at https://doi.org/10.1016/j.memsci.2024.122764.

References

[1] R.-M. Lu, Y.-C. Hwang, I.J. Liu, C.-C. Lee, H.-Z. Tsai, H.-J. Li, H.-C. Wu, Development of therapeutic antibodies for the treatment of diseases, J. Biomed. Sci. 27 (1) (2020) 1, https://doi.org/10.1186/s12929-019-0592-z.

[2] J. Dumont, D. Euwart, B. Mei, S. Estes, R. Kshirsagar, Human cell lines for biopharmaceutical manufacturing: history, status, and future perspectives, Crit. Rev. Biotechnol. 36 (6) (2016) 1110–1122, https://doi.org/10.3109/07388551.2015.1084266.

[3] L. Chu, D.K. Robinson, Industrial choices for protein production by large-scale cell culture, Curr. Opin. Biotechnol. 12 (2) (2001) 180–187, https://doi.org/10.1016/s0958-1669(00)00197-x.

[4] G. Walsh, Post-translational modifications of protein biopharmaceuticals, Drug Discov. Today 15 (17–18) (2010) 773–780, https://doi.org/10.1016/j.drudis.2010.06.009.

[5] A. Kantardjieff, W. Zhou, Mammalian cell cultures for biologics manufacturing, in: W. Zhou, A. Kantardjieff (Eds.), Mammalian Cell Cultures for Biologics Manufacturing, Springer Berlin Heidelberg, Berlin, Heidelberg, 2014, pp. 1–9, https://doi.org/10.1007/10_2013_255.

[6] O.B. McManus, M.L. Garcia, D. Weaver, M. Bryant, S. Titus, J.B. Herrington, Ion Channel Screening in: Assay Guidance Manual, Eli Lilly & Company and the National Center for Advancing Translational Sciences, 2012 [Internet].

[7] H.P. Erickson, Size and shape of protein molecules at the nanometer level determined by sedimentation, gel filtration, and electron microscopy, Biol. Proced. Online 11 (1) (2009) 32, https://doi.org/10.1007/s12575-009-9008-x.

[8] P. Romann, P. Giller, A. Sibilia, C. Herwig, A.L. Zydney, A. Perilleux, J. Souquet, J. M. Bielser, T.K. Villiger, Co-current filtrate flow in TFF perfusion processes: decoupling transmembrane pressure from crossflow to improve product sieving, Biotechnol. Bioeng. 121 (2) (2024) 640–654, https://doi.org/10.1002/bit.28589.

[9] M. Pappenreiter, H. Schwarz, B. Sissolak, A. Jungbauer, V.r. Chotteau, Product sieving of mAb and its high molecular weight species in different modes of ATF and TFF perfusion cell cultures, J. Chem. Technol. Biotechnol. 98 (7) (2023) 1658–1672, https://doi.org/10.1002/jctb.7386.

[10] D.J. Karst, E. Serra, T.K. Villiger, M. Soos, M. Morbidelli, Characterization and comparison of ATF and TFF in stirred bioreactors for continuous mammalian cell culture processes, Biochem. Eng. J. 110 (2016) 17–26, https://doi.org/10.1016/j.bej.2016.02.003.

[11] S. Wang, S. Godfrey, J. Ravikrishnan, H. Lin, J. Vogel, J. Coffman, Shear contributions to cell culture performance and product recovery in ATF and TFF perfusion systems, J. Biotechnol. 246 (2017) 52–60, https://doi.org/10.1016/j.jbiotec.2017.01.020.

[12] H.d. Hoog, B.M. Fernhout, M.v.d. Bergh, T. Kuijper, K. Tyczko, E. Pineda, Investigation of XCell ATF® perfusion technology for virus manufacturing process intensification at MSD animal health. https://www.repligen.com/Products/xcell-atf/technology/resources/white_paper/Animal_Vaccine_Mnfg_Whitepaper_20JUL2022.pdf, 2022. (Accessed 20 December 2023).

[13] F. Radoniqi, H. Zhang, C.L. Bardliving, P. Shamlou, J. Coffman, Computational fluid dynamic modeling of alternating tangential flow filtration for perfusion cell culture, Biotechnol. Bioeng. 115 (11) (2018) 2751–2759, https://doi.org/10.1002/bit.26813.

[14] X. Du, Y. Shi, V. Jegatheesan, I.U. Haq, A review on the mechanism, impacts and control methods of membrane fouling in MBR system, Membranes 10 (2) (2020), https://doi.org/10.3390/membranes10020024.

[15] W. Guo, H.-H. Ngo, J. Li, A mini-review on membrane fouling, Bioresour. Technol. 122 (2012) 27–34, https://doi.org/10.1016/j.biortech.2012.04.089.

[16] K.V. Peinemann, S.P. Nunes, Membranes for Water Treatment, ume 4, Wiley-VCH Weinheim, Weinheim, 2010.

[17] P. Bacchin, P. Aimar, R.W. Field, Critical and sustainable fluxes: theory, experiments and applications, J. Membr. Sci. 281 (1) (2006) 42–69, https://doi.org/10.1016/j.memsci.2006.04.014.

[18] R.W. Field, D. Wu, J.A. Howell, B.B. Gupta, Critical flux concept for microfiltration fouling, J. Membr. Sci. 100 (3) (1995) 259–272, https://doi.org/10.1016/0376-7388(94)00265-Z.

[19] P. van der Marel, A. Zwijnenburg, A. Kemperman, M. Wessling, H. Temmink, W. van der Meer, An improved flux-step method to determine the critical flux and the critical flux for irreversibility in a membrane bioreactor, J. Membr. Sci. 332 (1) (2009) 24–29, https://doi.org/10.1016/j.memsci.2009.01.046.

[20] B. Raghunath, B. Wang, P. Pattnaik, J. Janssens, Best practices for optimization and scale-up of microfiltration TFF processes, BioProc. J. 11 (2012) 30–40, https://doi.org/10.12665/J111.Raghunath.

[21] BioOptimal TM.MF-SL. AsahiKasei, Hollow fiber microfilter. https://planova.ak-bio.com/products_services/biooptimal/file/743/biooptimalmfsl_brochure_en.pdf, 2018. (Accessed 20 November 2023).

[22] R. Darby, Chemical Engineering Fluid Mechanics, Revised and Expanded, second ed., CRC Press, 2001 https://doi.org/10.1201/9781315274492. Taylor & Francis.

[23] A.H. Fischer, K.A. Jacobson, J. Rose, R. Zeller, Preparation of cells and tissues for fluorescence microscopy, in: D.L. Spector, R.D. Goldman (Eds.), Basic Methods in Microscopy : Protocols and Concepts from Cells : a Laboratory Manual, Cold Spring Harbor Laboratory Press Cold Spring Harbor, N.Y., 2006, pp. 103–122. Cold Spring Harbor, N.Y.

[24] A. Kádár, G.b. Wittmann, Z. Liposits, C. Fekete, Improved method for combination of immunocytochemistry and Nissl staining, J. Neurosci. Methods 184 (1) (2009) 115–118, https://doi.org/10.1016/j.jneumeth.2009.07.010.

[25] D.J. Karst, K. Ramer, E.H. Hughes, C. Jiang, P.J. Jacobs, F.G. Mitchelson, Modulation of transmembrane pressure in manufacturing scale tangential flow filtration N-1 perfusion seed culture, Biotechnol. Prog. 36 (6) (2020) e3040, https://doi.org/10.1002/btpr.3040.

[26] S.-C. Kim, S. An, H.-K. Kim, B.-S. Park, K.-H. Na, B.-G. Kim, Modified harvest system for enhancing Factor VIII yield in alternating tangential flow perfusion culture, J. Biosci. Bioeng. 121 (5) (2016) 561–565, https://doi.org/10.1016/j.jbiosc.2015.10.001.

[27] D. Zhang, P. Patel, D. Strauss, X. Qian, S.R. Wickramasinghe, Modeling flux in tangential flow filtration using a reverse asymmetric membrane for Chinese hamster ovary cell clarification, Biotechnol. Prog. 37 (3) (2021) e3115, https://doi.org/10.1002/btpr.3115.

[28] A. Guerra, G. Jonsson, A. Rasmussen, E. Waagner Nielsen, D. Edelsten, Low cross-flow velocity microfiltration of skim milk for removal of bacterial spores, Int. Dairy J. 7 (12) (1997) 849–861, https://doi.org/10.1016/S0958-6946(98)00009-0.

[29] M.F.M. ClinckeCarin, Y. Zhang, E. Lindskog, K. Walsh, V. Chotteau, Very high density of CHO cells in perfusion by ATF or TFF in WAVE bioreactor™. Part I. Effect of the cell density on the process, Biotechnol. Prog. 29 (3) (2013) 754–767, https://doi.org/10.1002/btpr.1704.

[30] M.F.M. ClinckeCarin, P.K. Samani, E. Lindskog, E. Fäldt, K. Walsh, V. Chotteau, Very high density of Chinese hamster ovary cells in perfusion by alternating tangential flow or tangential flow filtration in WAVE Bioreactor™-part II: applications for antibody production and cryopreservation, Biotechnol. Prog. 29 (3) (2013) 768–777, https://doi.org/10.1002/btpr.1703.

[31] J. Walther, J. McLarty, T. Johnson, The effects of alternating tangential flow (ATF) residence time, hydrodynamic stress, and filtration flux on high-density perfusion cell culture, Biotechnol. Bioeng. 116 (2) (2019) 320–332, https://doi.org/10.1002/bit.26811.

[32] W. Kelly, J. Scully, D. Zhang, G. Feng, M. Lavengood, J. Condon, J. Knighton, R. Bhatia, Understanding and modeling alternating tangential flow filtration for perfusion cell culture, Biotechnol. Prog. 30 (6) (2014) 1291–1300, https://doi.org/10.1002/btpr.1953.

[33] V. Sundar, D. Zhang, X. Qian, S.R. Wickramasinghe, J.P. Smelko, C. Carbrello, Y. Jabbour Al Maalouf, A.L. Zydney, Use of scanning electron microscopy and energy dispersive X-ray spectroscopy to identify key fouling species during alternating tangential filtration, Biotechnol. Prog. 39 (3) (2023) e3336, https://doi.org/10.1002/btpr.3336.